



**HAL**  
open science

## Observations on GEOS-1 of whistler mode turbulence generated by a ground-based VLF transmitter

T. Neubert, François Lefeuvre, Michel Parrot, N. Cornilleau-Wehrlin

► **To cite this version:**

T. Neubert, François Lefeuvre, Michel Parrot, N. Cornilleau-Wehrlin. Observations on GEOS-1 of whistler mode turbulence generated by a ground-based VLF transmitter. *Geophysical Research Letters*, 1983, 10 (8), pp.623-626. 10.1029/GL010i008p00623 . insu-03206518

**HAL Id: insu-03206518**

**<https://insu.hal.science/insu-03206518>**

Submitted on 23 Apr 2021

**HAL** is a multi-disciplinary open access archive for the deposit and dissemination of scientific research documents, whether they are published or not. The documents may come from teaching and research institutions in France or abroad, or from public or private research centers.

L'archive ouverte pluridisciplinaire **HAL**, est destinée au dépôt et à la diffusion de documents scientifiques de niveau recherche, publiés ou non, émanant des établissements d'enseignement et de recherche français ou étrangers, des laboratoires publics ou privés.

OBSERVATIONS ON GEOS-1 OF WHISTLER MODE TURBULENCE GENERATED BY A GROUND-BASED VLF TRANSMITTER

T. Neubert

Danish Space Research Institute, Lundtoftevej 7, DK-2800 Lyngby, Denmark

F. Lefeuvre, M. Parrot

LPCE/CNRS, 45045 Cedex, Orleans, France

N. Cornilleau-Wehrlin

CRPE/CNET, 92131 Issy-les-Moulineaux, France

**Abstract.** Signals launched by the NLK Jim Creek transmitter in Alaska on 18.60 and 18.65 kHz have been observed on GEOS-1. Data for one pass over Alaska on June 11, 1977, are presented here. The peak amplitude of the signals is  $\sim 5$  pT (0.6 mV/m), which is received when the satellite is close to exact conjugacy at 7500 km altitude. While the weaker signals received at some distance from conjugacy behave as expected from linear theory, the stronger signals received closer to conjugacy have features which indicate that some non-linear process is active. These features are: 1) a turbulent electric frequency spectrum 2) an increased electrostatic character of the waves. The threshold field amplitude of the supposed (but unidentified) non-linear interaction is  $\sim 1$  pT.

#### Introduction

Turbulence of ground based VLF transmitter signals received by low altitude satellites at conjugacy in the opposite hemisphere has been analyzed in Edgar [1976]. Here the observations are interpreted in terms of linear propagation effects, where large wave normal angles produce large Doppler shifts induced by the satellite motion. In the present case, the satellite and the transmitter are in the same hemisphere.

The observations are presented in a preliminary report by Cornilleau-Wehrlin et al. [1978]. They observe a puzzling feature, namely a depression in the  $cB/E$  ratio, where  $c$  is the velocity of light in vacuum, and  $B, E$  the magnetic and electric field amplitudes of the whistler waves. This occurs for high field values in the part of the orbit where the satellite is close to conjugacy with the transmitter. The depression is rather abrupt, the ratio falling to  $1/3$  of the values found in the border regions.

It is the purpose of the present paper to extend the analysis and discussion of Cornilleau-Wehrlin et al. [1978]. First the experimental set up is described, and the turbulent nature of the electric signal in the part of the orbit coinciding with the depression in the  $cB/E$  ratio is demonstrated. Then calculations of the polarization, ellipticity, and wave normal direction are presented. Finally the refractive

index and the propagation characteristics are discussed along with the amplitude calibration of the wave experiment. It is concluded that linear theory is inadequate for describing the observations. Some suggestions are made for further studies.

#### The Set Up

The Jim Creek signals are recorded by the Swept Frequency Analyzer system (SFA) on GEOS-1. Six SFA's operate as heterodyne systems controlled by a single frequency synthesizer. The analyzers select bands of 300 Hz in the frequency range 150 Hz to 77 kHz in 256 steps of 300 Hz, thus giving a complete coverage. The sampling frequency is 1488 Hz, and the bandwidth is determined by a highpass filter at 150 Hz and a low pass filter at 450 Hz. When recording the Jim Creek signals the SFA's were connected to three magnetic and three electric sensors. The sensors are parallel to the axis of a cartesian coordinate system with  $x, y$  in the spin plane and  $z$  along the spin axis. A more detailed description of the GEOS wave experiment is found in S-300 Experimenters [1978].

The SFA swept 4 steps around the transmitted frequencies, recording 0.69 s on each step (1024 samples). This scheme was followed in order to enable the detection of triggered emissions. Such emissions were, however, not observed, and the present paper uses SFA data from one step only, covering the frequency range 18.5 to 18.8 kHz.

The Jim Creek transmitter emits coded information switching between 18.60 and 18.65 kHz. The minimum duration on either frequency is 10 ms.

Two types of spectral analysis have been performed. One is a Fourier transform of the 1024 samples from each SFA, producing amplitude spectra with 1.4 Hz frequency resolution for each of the 6 wave field components. A spectrum calculated from a 0.69 s interval will then contain both frequency components including some sidebands. However, the strongest component in a spectrum will be on either 18.60 or 18.65 kHz if the rays reaching the satellite behave linearly, and the Doppler shift induced by the satellite motion is negligible.

The other method consists of the construction of  $3 \times 3$  spectral matrices of the magnetic field components, calculated from time averaged modified periodograms [Welch, 1967]. Depending on the time stationarity of the signal, intervals of

Copyright 1983 by the American Geophysical Union.

Paper number 3L0871.  
0094-8276/83/003L-0871\$03.00

0.52 to 0.60 s have been analyzed with a 23 Hz frequency resolution. This makes it impossible to discriminate between the two emitted frequencies. Since analysis with a better frequency resolution gives a poorer signal to noise ratio, it seems safer to assume that the waves on the two frequencies have the same propagation characteristics allowing them to mix in the analysis.

### Observations

The rms values of the magnetic and electric field amplitudes can be calculated from the amplitude spectra. They are shown versus time in Figures 1a and 1b. At 7.30 UT the satellite is approaching the Earth at 10,000 km altitude, and at 7.55 UT it is located at 5,000 km altitude, still descending (see Figure 1 of Cornilleau-Wehrlin et al., 1978). At 7.45 UT the satellite is at almost exact conjugacy at 7,500 km altitude as calculated from an Olson-Pfizer model [Kosik, 1978].

While the electric signal varies relatively smoothly, the magnetic signal has large amplitude variations with conspicuous peaks around 7.36 and 7.42 UT. Figure 1c shows the ratio  $cB/E$  as function of time. The ratio increases between 7.33 and 7.37 UT as the Jim Creek signal rises out of the noise. However, the ratio drops abruptly at 7.37 UT from  $\sim 4.5$  to  $\sim 2$  and decreases further until 7.52 UT where it suddenly rises from  $\sim 1$  to  $\sim 3$ . An exception is the peak at 7.42 UT.

For parallel propagating whistler mode waves the refractive index is given by  $cB/E$ . The values shown in Figure 1c are, within the depression region, a factor 4-6 times lower than expected from theory (see Discussion).

The occurrence of the frequency of the maximum amplitude component in each of the  $\sim 700$  spectra calculated from 7.25 to 8.00 UT is shown in

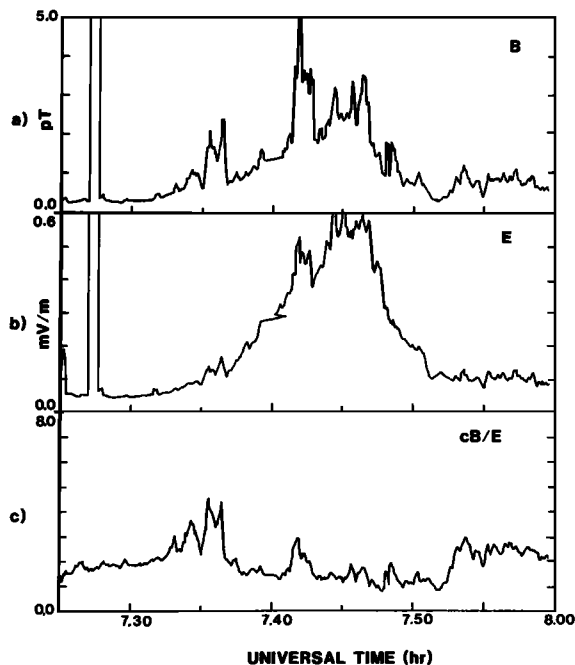


Figure 1. a) Amplitude of the magnetic field b) amplitude of the electric field c)  $cB/E$ .

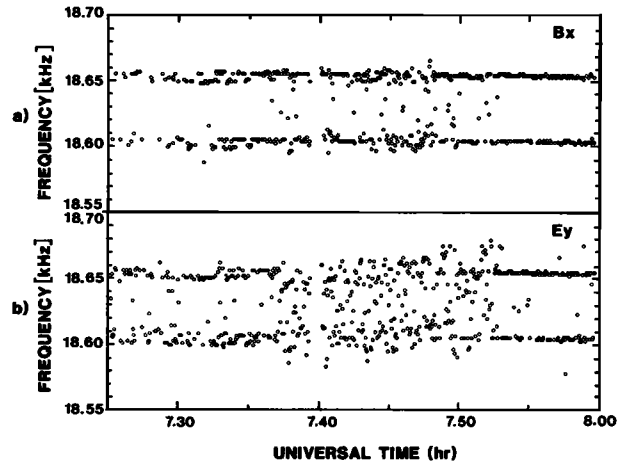


Figure 2. Occurrence of strongest frequency component

Figure 2. From 7.37 to 7.52 UT a few spectral points on Bx appear in between the transmitted frequencies, signifying a modest state of turbulence.

The signal on Ey behaves different from that on Bx in the period 7.37 to 7.52 UT, which coincides exactly with the period of depression in  $cB/E$ . The signal is very turbulent, the maximum spectral component appearing anywhere from 20 Hz below the lower to 30 Hz above the upper of the two transmitted frequencies.

The noisy nature of the signals is illustrated further in Figure 3. Spectra averaged over 5 min are shown for three time intervals: 7.32 - 7.37 UT (not noisy), 7.47 - 7.52 UT (noisy), and 7.53 - 7.58 UT (not noisy). The spectra from Bx and Ey are similar in the periods that are not noisy, and resemble spectra calculated from simulated signals. In the noisy period, the Bx spectrum is slightly changed, while the Ey spectrum is very turbulent.

The double peaks on Bx and Ey with a  $\sim 5$  Hz frequency separation seen on the spectra from 7.32 - 7.37 UT are believed to be an effect caused by two raypaths leading to the satellite in the 5 min period. The wave normal angle of the rays at the location of the satellite differ and the rays experience different Doppler shifts. Inspection of individual spectra and Figure 2 indicate that the two ray paths exist simultaneously.

As a final point in this section the ellipticity, polarization, and wave normal direction will be investigated. A detailed analysis is not possible since measurements of the Earth magnetic field  $B_0$ , and the plasma frequency  $f_p$  do not exist. Still, some indications can be obtained from model estimates. Thus  $B_0$  is estimated from a Magsat (6/80) model [Langlet et al., 1980], while  $f_p$  is taken from Chiu et al. [1979].

The 4 step cycle of the SFA has a 2.75 s period, while the satellite spin has a 5.7 s period. The satellite then rotates  $43.4^\circ$  during one step, while the orientation of the xy-antennas is shifted  $173.8^\circ$  each 4 step cycle. For a signal elliptically polarized in the xy plane, this results in an amplitude modulation with a period of 80 s.

The ellipticity of the magnetic wave field in the xy plane at the upper transmitted frequency is found from the rms amplitudes measured on Bx and By in a 14 Hz band at 18.65 kHz. Using the fact that the magnetic field of a plane whistler mode wave is circularly polarized in the plane perpendicular to the wave normal  $\underline{k}$ , the angle of  $\underline{k}$  to the satellite spin axis can be found. The result is the curve marked x, shown in Figure 4a. The points connected with dashed lines suffer from uncertainties due to irregular fluctuations in Bx/By. The same procedure can be used with the signals on Bx and Bz. The result is the curve marked o in Figure 4a. The analysis is confined to the time interval 7.33 to 7.55 UT where the Jim Creek signal is predominant.

While the angle to the spin axis may be calculated by the two methods outlined above, the azimuth angle is still unknown. The discrepancy shown in Figure 4b is then just an indication of whether the wave field averaged over 40 s may be considered as plane. This seems to be the case around 7.42 UT and from 7.48 to 7.55 UT.

The results of Figure 4 are to be compared with the angle of  $\underline{B}_0$  to the spin axis of the satellite. At 7.30 UT the angle is  $75^\circ$ , decreasing to  $71^\circ$  at 7.51 UT. Thus, the smallest possible wave normal angle to  $\underline{B}_0$  for the periods of plane waves can be estimated to be  $\sim 5^\circ$  at 7.42 UT and  $\sim 15^\circ$  from 7.48 to 7.55 UT.

The polarization of the magnetic field changes at 7.48 UT which is still in the period of turbulence. This behaviour is different from that of the electric field polarization as measured in the xy plane which is well defined during the whole period where the Jim Creek signal is dominant. The average ellipticity is around 0.5 and unaffected by the degree of turbulence.

The polarization P and ellipticity E have been estimated from 3 x 3 spectral matrices of the magnetic field components [Samson and Olson, 1980] at 66 time intervals in the period 7.32 to 7.53 UT. The wave field can be regarded as that of one plane wave if  $P > 0.9$ , while the ellipticity of plane whistler mode waves is expected to be close to 1 [Lefeuvre et al., 1982].

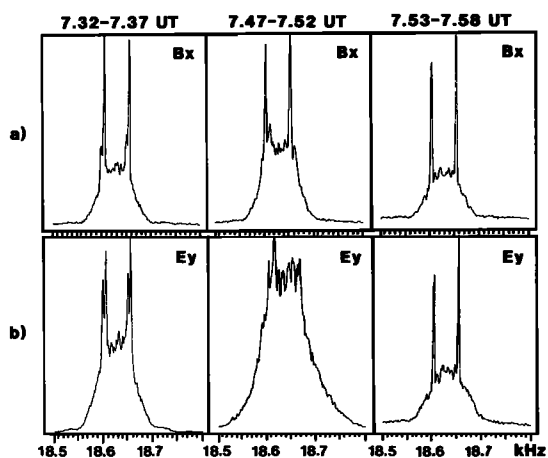


Figure 3. Averages of spectra (normalized relative to peak amplitude).

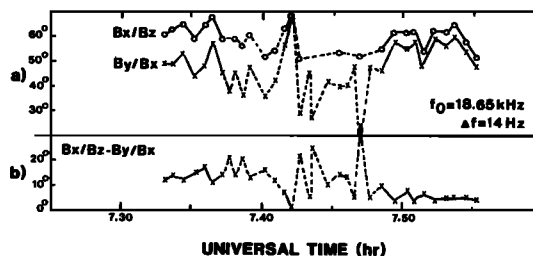


Figure 4. a) Angle of wave normal to the satellite spin axis b) difference in results of the two methods used in a).

Only 7 cases have  $P > 0.9$ . These are grouped around 7.36, 7.42 and 7.48 UT, and coincide with three of the peaks in the magnetic field amplitude (Figure 1a). Note also that they fall within the regions of well determined polarization of Figure 4a (solid lines). Furthermore, in 16 cases the analysis shows that the wave field is left hand polarized, in contradiction to theory, which predicts right hand polarization.

In Lefeuvre et al. [1982] it was concluded that the wave normal direction derived from a spectral analysis is believable only for  $E > 0.6$ . Just one case, at 7.36 UT, meets this requirement. Here a one peak Wave Distribution Function [Storey and Lefeuvre, 1979] is found, and the angle of  $\underline{k}$  to the satellite spin axis determined by Means method [Means, 1972] is  $73^\circ$ , in reasonable agreement with the results in Figure 4a.

Two peak WDF's are obtained at 7.32 and 7.41 UT. The solutions are acceptable since the angles of the wave normal to the spin axis derived from the measured matrices (by Means method) are almost identical to the ones found from the matrices reconstructed from the WDF solutions. Also a two peak WDF is consistent with the low value of P and E found in these cases.

Discussion

The refractive index  $\mu$  of whistler mode waves may be expressed on the form:  $\mu_1 = f_p \sqrt{f(f_c \cos \theta - f)}$ . Here f is the wave frequency,  $f_p, f_c$  the electron plasma and gyro frequencies, and  $\theta$  the angle  $\underline{k}, \underline{B}_0$ . With model estimates of  $f_c$  [Langel et al., 1980] and  $f_p$  [Chiu et al., 1979], refractive index estimates are calculated and listed in Table 1 for  $\theta = 0^\circ$  and  $60^\circ$  at three times. In the table is also listed the maximum expected Doppler shift  $\Delta f_m = kv_s/2\pi$ , where  $v_s$  is the satellite velocity.

Outside the depression region, the measured frequency shift is  $\sim +5$  Hz (Figure 3), which is consistent with the model estimate of the Doppler shift.

The refractive index  $\mu_2$  of electromagnetic waves is given by:  $\mu_2 = cB/E_\perp$  where  $E_\perp$  is the component of the electric field perpendicular to the wave normal  $\underline{k}$ . For parallel propagating waves ( $\theta = 0^\circ$ )  $E_\perp = E$ , and a plot like the one in Figure 1c would in this case be a direct measure of the refractive index. In general  $\theta \neq 0^\circ$  and as  $E_\parallel/E_\perp = \sin \theta / (\cos \theta - f/f_c)$ , the ratio  $cB/E$  will in general be smaller than the refractive index.

The refractive index for parallel propagation expected from the model is a factor 2 larger

Table 1. Model estimates for three satellite locations.

Time (UT)	7.35	7.45	7.55
Altitude (km)	9300	7200	5000
$f_p$ (kHz)	260	300	370
$f_c$ (kHz)	80	120	200
$\mu_1$ ( $\theta=0^\circ$ )	7.8	7.0	6.5
$\mu_1$ ( $\theta=60^\circ$ )	13.1	10.9	9.6
$v_s$ (km/s)	7.7	8.9	10.1
$\Delta f_m$ ( $\theta=0^\circ$ ) (Hz)	3.6	3.7	3.9
$\Delta f_m$ ( $\theta=60^\circ$ ) (Hz)	6.1	5.8	5.8

than the ratio  $cB/E$  of Figure 1c in the periods bordering the depression, and a factor 4-6 larger within that region. The model parameters are thought to be reasonable since June 11 was in a magnetically quiet period with  $K_p < 2$  during the previous 24 hours, and GEOS was inside the plasmapause. Several possibilities are then open: the amplitude measurements are erroneous, the waves propagated with very oblique wave normals, and/or the signals behave non-linearly.

The possibility of errors in the calibration of the electric antennas is discussed in Neubert et al. [1982], which concludes that the electric field amplitudes may be overestimated by a factor 2 to 6, and in Lefeuvre et al. [1982], which arrive at a factor 3.5.

A factor 2 larger  $cB/E$  ratio seems to be consistent with refractive index estimates in the regions bordering the depression and at 7.42 UT. With the results of the ellipticity and polarization study it is then concluded that the signals in these regions behave linearly.

Within the depression region the high degree of turbulence and the electrostatic character of the waves are consistent with waves propagating with wave normals very close to the resonance cone, the frequency being Doppler shifted by the satellite motion (turbulent propagation vector spectrum). However, it is not possible to identify the responsible scattering mechanism since the data set is rather limited. The wave amplitudes are so large that even local non-linear wave-wave interactions may be possible [Neubert, 1982]. If this is the case the threshold field read from Figure 1 is  $\sim 1$  pT.

We suggest that ISEE-1 and -2 VLF data for passes near the Aldra Omega station be analyzed. It should be possible to derive the refractive index for the 10.2 kHz transmissions.

**Acknowledgments.** We wish to thank T. Bell for his helpful suggestions and the information

on the plasma pause position. This work was supported in part by the Danish Space Board, Danish Natural Science Research Council, and the Otto Mønsted Foundation.

#### References

- Chiu, Y.T., J.G. Luhmann, B.K. King, and D.J. Butcher Jr., An equilibrium model of plasmasphere composition and density, *J.Geophys.Res.*, **84**, 909-916, 1979.
- Cornilleau-Wehrin, N., R. Gendrin, and R. Perez, Reception of the NLK (Jim Creek) transmitter onboard GEOS-1, *Space Sci. Rev.*, **22**, 443-451, 1978.
- Edgar, B.C., The theory of VLF Doppler signatures and their relation to magnetospheric density structures, *J.Geophys.Res.*, **81**, 3327-3339, 1976.
- Kosik, J.C., The use of past and present magnetospheric field models for mapping fluxes and calculating conjugate points, *Space Sci. Rev.*, **22**, 481-497, 1978.
- Langel, R.A., R.H. Estes, G.D. Mead, E.D. Fabiano, and E.R. Lancaster, Initial geomagnetic field model from MAGSAT vector data, *Geophys.Res.Lett.*, **7**, 793-796, 1980.
- Lefeuvre, F., T. Neubert, and M. Parrot, Wave normal directions and wave distribution functions for ground-based transmitter signals observed on GEOS-1, *J.Geophys.Res.*, **87**, 6203-6217, 1982.
- Means, J.D., The use of the three dimensional covariance matrix in analyzing the properties of plane waves, *J.Geophys.Res.*, **77**, 5551-5559, 1972.
- Neubert, T., Stimulated scattering of whistler waves by ion acoustic waves in the magnetosphere, *Physica Scripta*, **26**, 239-247, 1982.
- Neubert, T., E. Ungstrup, and A. Bahnsen, Observations on the GEOS-1 satellite of whistler mode signals transmitted by the Omega navigation system transmitter in northern Norway, *J.Gephys.Res.*, **88**, 4015-4025, 1983.
- Samson, J.C., and J.V. Olson, Some comments on the description of the polarization-states of waves, *Geophys.J.R.Astron.Soc.*, **61**, 115-129, 1980.
- Storey, L.R.O., and F. Lefeuvre, Analysis of a wave field in a magnetoplasma, 1-the direct problem, *Geophys.J.R.Astron.Soc.*, **56**, 255-270, 1979.
- S-300 Experimenters, Measurements of electric and magnetic wave fields and of cold plasma parameters on-board GEOS-1, preliminary results, *Planet.Space Sci.*, **27**, 317-339, 1979.
- Welch, P.D., The use of fast Fourier transform for the estimation of power spectra: A method based on time averaging over short, modified periodograms, *IEEE Trans. Audio Electroacoust.*, **15**, 70-73, 1967.

(Received March 14, 1983;  
accepted May 18, 1983.)